Verification of Back Stress in a Constitutive Model for Cyclic Plasticity

H. ISHIKAWA
Hkokkaido University, Sapporo, Japan

ABSTRACT

Aiming at a formulation of the unified constitutive model of cyclic plasticity and creep, the concept of the effective stress which is defined as stress measured from the current center of yield surface, is employed to explain the intermittent creep period after cyclic prestraining. Then the experimental results show a marvelous regularity which might make us easily to construct the unified constitutive model.

1 INTRODUCTION

The authors have recently proposed the constitutive model of cyclic plasticity (Ishikawa and Sasaki 1988), where the following four important assumptions were employed: (1)The plastic-deformation-induced anisotropy and the motion of the center of the loading surface were incorporated in the yield function. (2)The associated plastic flow law was derived from the so called normality of the plastic strain increments to the yield surface. (3)The Ziegler type of kinematic hardening was used as the evolution equation of the center of the loading surface. (4)All the stress-strain curves in cyclic loading were also assumed to be represented well by the modified Ramberg-Osgood law which should be applied from the current center of the loading surface. Assumptions (1),(2) and (4) have been verified already from the experiments (Ishikawa and Sasaki 1988, 1989).

Consequently, only one assumption which should be verified, is the Ziegler type of kinematic hardening, i.e. the evolution of back stress, which has attracted the interest of researchers in relation to ratchetting. In this paper, the concept of the effective stress which is defined as stress measured from back stress, is employed to explain the intermittent creep period after cyclic prestraining. Then the experimental results show a marvelous regularity, similarly as might be reminded easily of the regular shapes of the equi-plastic-strain surface probed at back stress (Ishikawa and Sasaki 1989). These interesting facts show the indirect verification of the exact trace of the evolution of back stress.

SMiRT 11 Transactions Vol. L (August 1991) Tokyo, Japan, © 1991

2 EXPERIMENT

2.1 Testing Equipments and Procedure

The specimens used in this work have the gauge length of 50mm, and the inner and outer radii of the tube of 20mm and 23mm, respectively. The specimens were made of type 304 stainless steel subjected to heat treatment at 1070 °C, its chemical compositions were 0.06C, 0.51Si, 1.06Mn, 0.028P, 0.012S, 8.81Ni, 18.38Cr, and Fe balance in weight percent. Young's modulus at room temperature was equal to E=198GPa, while shearing modulus G=73.5GPa.

A servocontrolled axial-torsion testing machine (Shimadzu EHF-EB10) together the Shimadzu 4825 controller and a computer (NEC PC-9801VM) was used for computerized testing and data acquisition accomplished by a program written in Machine Word. Strains measured using two strain gauges applied on diametrically opposite sides of the specimens or an extensometer. The axial force were measured using a load cell incorporated in the machine. The stress controlled mode was used for cyclic plasticity and creep test. With the aid of the computer system, the constant stress rate $\dot{\sigma}$= 10 (MPa/sec) was maintained during plastic loading, and the resulting stress-strain responses were recorded on a floppy-disk by the computer. A data point was recorded whenever the stress changed by 5 MPa.

2.2 Creep behavior at the same stress level during uniaxial loading

A stress-strain diagram of a specimen which was subjected to creep tests during uniaxial loading with the stress rate $\dot{\sigma}$= 10 (MPa/sec) is given in Fig.1. Creep strains AB(=0.19%) and EF(=0.0%) are obtained after same time intervals of 300 sec under the same stress level of 240 MPa. The difference of creep strains between AB and EF may be caused by a structural change in the internal variable during unloading DE. What kind of internal variable governs this phenomenon? It should be worth seeking for a constitutive modeling of cyclic viscoplasticity. The similar problem concerned will be discussed in the following section. In addition, it is important to note that upon a further tensile under stress controlled loading with the same stress rate $\dot{\sigma}$= 10 (MPa/sec), BCD, or FGH, the material continues to harden as in a regular tensile test, and the dashed extension emanating from A or D in Fig.1 is the curve for an uninterrupted tensile test. This phenomenon seems to give the important suggestion on an interaction between plastic strain and creep strain.

2.3 Creep during Cyclic loading

The experimental results were obtained in a quasi-cyclic-steady state. Namely, specimens were subjected to stress-controlled cycling with the stress rate $\dot{\sigma}$=10 (MPa/sec) at the strain amplitude of $\Delta\bar{\varepsilon}$=1.1%, until the hysteresis loops were stable. Creep periods were then introduced around the loops and the creep behavior was obtained.

Figure 2 shows the intermittent creep periods of 300sec duration during strain cycling between ±0.55%. After stabilization of cyclic straining with the 5th cycle, the creep periods start at the point a. All consecutive creep-hold periods are designated by alphabet letters ending at k. In spite of the same stress levels at a and j, b and i, d and g, and at e and f, creep in the nearly straight sections of the hysteresis loop is very small or nonexistent. At c and h, which are points of zero stress, the magnitude of strain decreases by a small but noticeable amount. Due to the conventional creep theory, the creep rate depends on stress and time in the time-hardening theory or on stress and creep strain in the strain-hardening one. The results shown in Fig.2, however, are at variance with these theories. The additional observation of the results in Fig.2 shows that at the maximum stress level of the cycle the greatest amount of creep is found which subsequently subsides and then increases in the opposite direction as the curvature of the stress-strain curve increases. Therefore, a point of zero creep must exist by continuity arguments. However, this point of zero creep can not very well defined only from Fig.2 (Kujawski et al. 1980).

It is very reasonable that the origin of the stress space should move due to the plastic deformation as presented in many constitutive models for cyclic plasticity proposed presently; namely, the current center of yield surface, i.e., kinematic back stress evolved during cyclic preloading. The physical instinct shows that the point of zero creep should corresponds to this current center of yield surface. Nevertheless, the point of zero creep can not defined yet from an experiment because back stress is an internal variable. The author has succeed in defining the evolution of back stress from the computer simulation based on his constitutive modeling of cyclic plasticity (Ishikawa and Sasaki 1988,1989). Especially it was a very

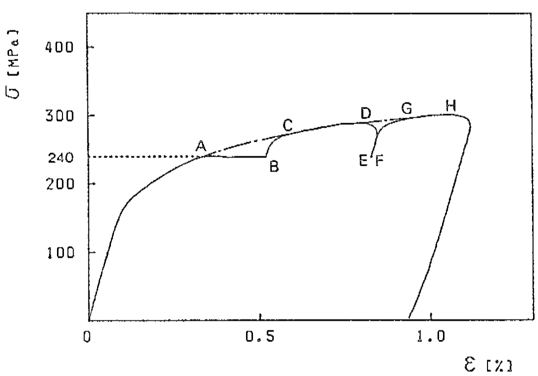

Fig.1 Creep behavior at the same stress level during uniaxial loading

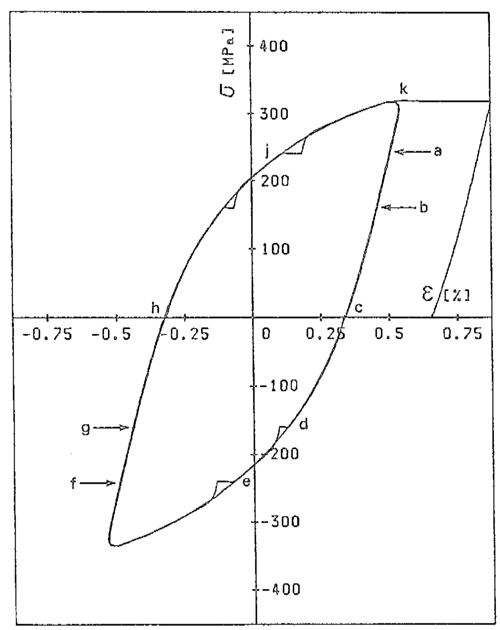

Fig.2 Intermittent creep periods of 300sec during cycling between ± 0.55%

interesting fact that the shape of the equi-plastic-strain surfaces, among which the yield surface was confined to the surface determined from proof strain of 50μm/m, could be described by a regular ellipse if it were probed at simulated back stress, while the equi-plastic-strain surface has a deformed shape with a rounded nose and a flatten back at the zero stress state unloaded completely (Ishikawa and Sasaki 1988).

3 SIMULATION

A brief summary of the mathematical structure of the hybrid constitutive model is reproduced from (Ishikawa and Sasaki 1988). Combining the Mises type stress-hardening with the kinematic hardening, the following yield function (1) is chosen for cyclically stable materials at temperature T. The associated flow low is derived from the normality of the plastic strain increments to the yield surface and is given by equation (2). Using Ziegler type of assumption as the evolution equation of the center of the loading surface, the motion of the center is given by equation (3).

$$f = \frac{1}{2} C_{ijkl} (\sigma_{ij} - \sigma^c_{ij}) (\sigma_{kl} - \sigma^c_{kl}) - \frac{1}{3} R^2 (\kappa , T) = 0 \tag{1}$$

$$d\varepsilon^p_{ij} = \frac{3 d\bar{\varepsilon}^p}{2R} C_{ijkl} (\sigma_{kl} - \sigma^c_{kl}) \tag{2}$$

$$d\sigma^c_{ij} = \frac{3}{2R^2} [C_{klmn} (\sigma_{mn} - \sigma^c_{mn}) d\sigma_{kl}] (\sigma_{ij} - \sigma^c_{ij}) - (\frac{dR}{dW^p}) (\sigma_{ij} - \sigma^c_{ij}) d\bar{\varepsilon}^p \tag{3}$$

In equations (1)-(3), C_{ijkl} is the plastic-deformation-induced anisotropy coefficient tensor of 4th rank, and σ_{ij} is stress. σ^c_{ij} is kinematic back stress, giving the translation of the yield surface. R is isotropic flow stress, describing the increase or decrease of the size of the yield surface, and κ is the hardening or softening parameter. Moreover, $d\varepsilon^p_{ij}$ and $d\bar{\varepsilon}^p$ are the plastic strain and the equivalent plastic strain increments.

All the stress-strain curves are assumed to be represented by the modified Ramberg-Osgood law (4).

$$\varepsilon_{ij} - \varepsilon^c_{ij} = \frac{\sigma_{ij} - \sigma^c_{ij}}{E} [1 + K \{ \frac{\bar{\sigma}}{\sigma_o} \}^m] \tag{4}$$

where E is Young's modulus, K is material constant, and $\bar{\sigma}$ is the equivalent stress. The quantities $\sigma_{o(n)}$ and $m_{(n)}$ in equation (4) are the reference stress at the proof strain ε_o =500 μm/m, and the exponent of hardening or softening after the (n-1)th inversion of loading, and they depend on the modified plastic work according to equation (5)-(6). R can be provided by equation (7) following equation (5).

$$\sigma_o = \sigma_{o(\infty)} [1 \mp \alpha \exp \{ - \frac{W^p_{(n-1)}}{W_o} \}] \tag{5}$$

$$m = m_{(\infty)} [1 \mp \beta \exp \{ - \frac{W^p_{(n-1)}}{W_1} \}] \tag{6}$$

$$R = R_{(\infty)} [1 \mp \lambda \exp \{ - \frac{W^p}{W_2} \}] \tag{7}$$

$\sigma_{o(\infty)}$, α, W_o, $m_{(\infty)}$, β, W_1, $R_{(\infty)}$, λ, and W_2 in equations (5)$\sim$(7) are constants prescribed by the history of loading or effected by a strain path memory. W^p in equation (7) is the accumulated plastic work which is equal to $W^p = W^p_{(n-1)} + \Delta W^p$ with the modified plastic work increment ΔW^p during loading in the current stage of deformation.

In the previous work (Ishikawa and Sasaki 1989), the yield function f in equation (1) was confirmed to be an adequate form for cyclic plasticity and the associated flow law given by equation (2) was also appreciated to be acceptable from the normality of the plastic strain increment vector to the subsequent yield surface. In addition, applicability of the Ramberg-Osgood law to the subsequent loading after cyclic loading is confirmed in (Ishikawa and Sasaki 1988). $\sigma_{o(1)}$=223MPa, $\sigma_{o(2)}$=250MPa, $m_{(1)}$=6.7, and $m_{(2)}$=3.7 can be evaluated directly from the experimental results, among which the stabilized stress-strain loop is shown in Fig.2. After several trials with the computer(NEC PC-9801VM), the simulated stress-strain curves shown by the solid lines in Fig.3 are depicted using $\sigma_{o(\infty)}=R_{(\infty)}$=275MPa, $\alpha=\lambda=0.07$, $W_o/\sigma_{o(\infty)}=W_2/\sigma_{o(\infty)}=0.10$, $m_{(\infty)}=3.3$, $\beta=0.13$ and $W_1/\sigma_{o(\infty)}=0.028$. The movement of the center of the yield surfaces during cyclic loading is traced by the dash-dot lines in Fig.3. The value of kinematic back stress during compression in the stabilized stress-strain loop is 160MPa. The stress at the point b in Fig.2 corresponds to this back stress, and therefore, the effective stress is defined in this work as stress measured from the points b or g, corresponding compression side of the stress-strain loop or tension one, respectively.

The creep curves corresponded to Fig.2 are given in Fig.4, where the absolute values of total strain measured from the point b or g is plotted during 300sec. The numerals in Fig.4 represent the effective stress.

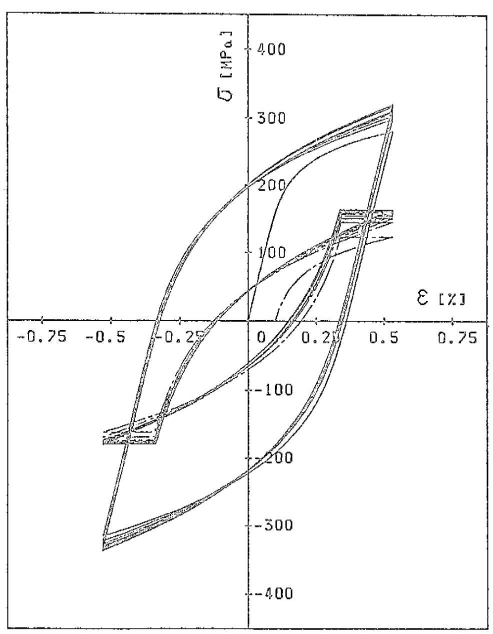

Fig.3 Cyclic tension-compression loading with strain amplitude of 1.1%

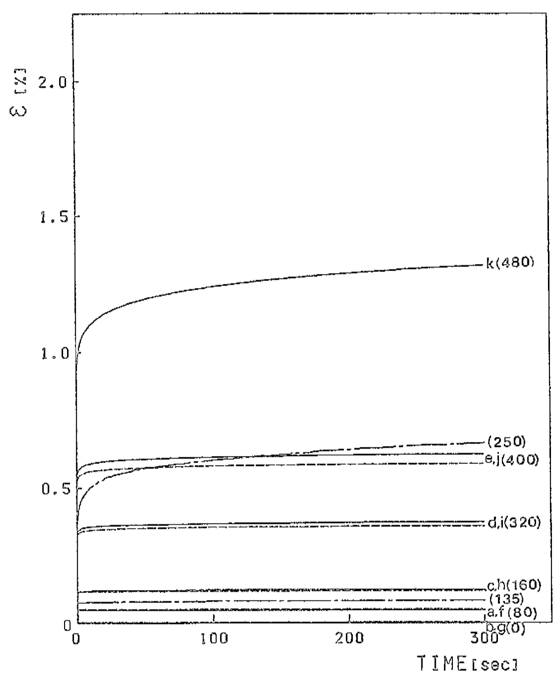

Fig.4 Total strain versus time for creep tests depicted in Figs.1 and 2

The solid lines show the creep along the tension side of the stress-strain loop, while the broken ones along the compression side. Two creep curves under the same stress level have a good agreement. This observation shows that the creep-rate depends on stress and time if stress is measured from the current center of loading surface as the conventional creep theory. Therefore, the evolution of back stress during cyclic preloading plays the important role to prescribe the following creep behavior. The creep curves corresponded to Fig.1 are also shown in Fig.4 by dash-dot lines. the numerals on the dash-dot lines represent also the effective stresses measured from the current centers of the stress space. The clear difference between creep during monotonic loading shown by dash-dot line and that during cyclic loading shown by solid or broken line represents the effect of cyclic plasticity, or fatigue on following creep behavior.

From the experimental results of creep during cyclic loading, the following conventional creep law has been obtained,

$$\varepsilon^c = 1.90 \times 10^{-5} \sigma^{1.72} t^{0.0181} \qquad (8)$$

where σ is the effective stress measured from the current center of yield surface, and t is time in second. This equation (8) is the so-called Bailey-Norton law.

4 CONCLUSION

To aim at a formulation of the unified constitutive model of cyclic plasticity and creep, the concept of effective stress which is defined in this paper as stress measured from the current center of yield surface, is employed to explain the intermittent creep period after cyclic prestraining. Then the creep behavior around the hysterisys loop of cyclic plasticity can be described by a conventional theory of creep. However, the cyclic plasticity in out-of-phase loading as mechanical ratchetting should be carefully examined to construct an unified theory.

REFERENCES

Kujawski, D., Kallianpur, V., and Kremple, E. (1980). An Experimental Study of Uniaxial Creep, Cyclic Creep and Relaxation of AISI Type 304 Stainless Steel at Room Temperature, J. Mech. Phys. Solids, Vol.28, pp.129-148.

Ishikawa, H., and Sasaki, K. (1988). Yield Surfaces of SUS304 under Cyclic Loading, ASME Journal of Engineering Materials and Technology, Vol.110, pp.364-371.

Ishikawa, H., and Sasaki, K. (1989). Stress-Strain Relations of SUS304 Stainless Steel After Cyclic Preloading, ASME Journal of Engineering Materials and Technology, Vol.111, pp.417-423.